

# RSC Advances



This is an *Accepted Manuscript*, which has been through the Royal Society of Chemistry peer review process and has been accepted for publication.

*Accepted Manuscripts* are published online shortly after acceptance, before technical editing, formatting and proof reading. Using this free service, authors can make their results available to the community, in citable form, before we publish the edited article. This *Accepted Manuscript* will be replaced by the edited, formatted and paginated article as soon as this is available.

You can find more information about *Accepted Manuscripts* in the [Information for Authors](#).

Please note that technical editing may introduce minor changes to the text and/or graphics, which may alter content. The journal's standard [Terms & Conditions](#) and the [Ethical guidelines](#) still apply. In no event shall the Royal Society of Chemistry be held responsible for any errors or omissions in this *Accepted Manuscript* or any consequences arising from the use of any information it contains.

# Design, preparation and characterization of novel toughened epoxy asphalt based on vegetable oil derivative for bridge deck paving

Shouhai Li <sup>a,b</sup>, Kun Huang <sup>a,b</sup>, Xuejuan Yang <sup>a</sup>, Mei Li <sup>a</sup>, Jianling Xia <sup>a,b,\*</sup>

<sup>a</sup>Institute of Chemical Industry of Forestry Products, CAF; Key Lab. of Biomass Energy and Material, Jiangsu Province; National Engineering Lab. for Biomass Chemical Utilization; Key and Lab. on Forest Chemical Engineering, SFA, Nanjing 210042, China

<sup>b</sup>Institute of Forest New Technology, CAF, Beijing 100091, China

\*Corresponding author e-mail: xiajianling@126.com

## Abstract:

The aim of this work was to prepare a series of novel toughened epoxy asphalt materials using natural oil derivative as main raw material for bridge deck paving. A polymerized fatty acid (PFA) epoxy curing agent was prepared from epoxy fatty acid methyl ester (EFAME) via catalytic ring-opening polymerization and hydrolyzation. Then the novel toughened epoxy asphalt materials with different weight ratios of PFA were prepared. Mechanical tests showed that the prepared toughened epoxy asphalt materials had excellent flexible tensile properties. Micro-morphologic investigation displayed the asphalt was dispersed more evenly with the increased PFA content, indicating excellent compatibility between the PFA cured system and asphalt. Dynamic mechanical analysis results showed two phases in the cured compositing system, and the changing trend of  $T_g$  indicates the excellent compatibility between the PFA cured system and asphalt. Comprehensive properties comparison showed that all performance parameters of our

prepared toughened curing system met the technical requirements for bridge deck paving. Curing behavior research showed that the  $E_a$  of the optimal toughened mixed epoxy asphalt curing system was higher and close to the value of pure epoxy curing system without asphalt.

**Key words:**

Epoxy fatty acid methyl ester; Catalytic polymerization; Polymerized fatty acid; Toughened epoxy asphalt; Comprehensive properties

**1. Introduction**

As an important building material, asphalt plays a critical role in many industries because of its excellent water resistance, chemical resistance and bondability.<sup>1-3</sup> With its huge output and popular price, asphalt material is widely used in road pavement, waterproof construction and shock absorption.<sup>4,5</sup> However, because of its thermoplastic properties, pure asphalt material performs poorly at high and low temperatures, and thus it is prone to deformation or crack at too high or too low temperature.<sup>6,7</sup> The durability of prepared asphalt pavement using pure asphalt material is greatly influenced by the environmental changes. These intrinsic defects restrict pure asphalt material from wide application, and the problems of stress and deformation inhibit its use in pavements on bridges.

In last four decades, thermosetting or thermoplastic polymer-modified asphalt materials with predominant performances have attracted much attention.<sup>8,9</sup> The polymer could form a continuous network within the asphalt, which improves the resistance against permanent deformation, thermal cracking and moisture damage, decreases the

temperature susceptibility of asphalt materials and increases the mechanical strength of asphalt. To reduce its performance deficiency, various polymer modifiers for asphalt have been developed,<sup>10</sup> such as epoxy resin, styrene butadiene styrene (SBS),<sup>11</sup> styrene butadiene rubber (SBR),<sup>12</sup> ethylene vinyl acetate (EVA)<sup>13</sup> and polyethylene (PE)<sup>14</sup>. Among them, thermosetting epoxy asphalt has received much attention and broad investigation because of its lower temperature susceptibility and higher mechanical strength, and thus it can be easily prepared and widely applied.<sup>15,16</sup>

Nevertheless, in an uncured mixed epoxy asphalt system, the asphalt and epoxy curing system tend to separate from each other because the poor compatibility reduces the stability of their performances.<sup>17,18</sup> Therefore, the compatibility between epoxy resin, curing agents and asphalt need to be improved. Modification of asphalt is an effective way to improve miscibility, such as maleated asphalt which can be cured by epoxy resin to improve the compatibility between asphalt and epoxy resin.<sup>19</sup> While we think choosing the proper curing agents of epoxy resins is a more effective way to improve miscibility

The matrix material of ordinary epoxy asphalt contains abundant rigid benzene molecular structures, and thus the epoxy asphalt provides high compressive strength and excellent antiabrasion properties.<sup>20</sup> However, for deck paving materials used in steel bridge structures, we need superior tensile properties, such as long breaking elongation. Thus, how to improve miscibility and tensile properties of epoxy asphalt mixtures efficiently has become a very attractive topic in the field of road materials.

Nowadays, great attention has been paid to exploring new polymers from renewable

resources that can replace petroleum-based products from the prospects of depletion of fossil fuels and protection of environment.<sup>21,22</sup> Many efforts have been devoted to formulating and preparing new polymers from agricultural and forestry feedstock.<sup>23,24</sup> The utilization of agricultural and forestry resources in polymer production might be considered as the most reasonable way to weaken environmental pollution as well as our dependence on fossil fuel.<sup>25</sup> Vegetable oil is an important agricultural resource and its molecule contains several particularly active functional groups (e.g. unsaturated double bonds and ester groups) that can be used for polymerization.<sup>26,27</sup> Vegetable oil resource is expected to be an ideal alternative to chemical feedstock. Epoxy fatty acid methyl ester (EFAME) is derived from oil, and its molecule contains multiple reactive functional epoxy groups. With its huge output and popular price, EFAME can serve as a natural and renewable plasticizer, dispersing agent, compatilizer, softener and surfactant.<sup>28-30</sup> The last decade has witnessed rapid development in the use of EFAME, as reported by several research teams.

E51, a bisphenol A-based epoxy resin, has been applied in various fields because of its relatively low price. Methyl tetrahydrophthalic anhydride (MTA), a very common epoxy curing agent, has great application potential in epoxy asphalt because of its applicable curing temperature with epoxy resin. However, E51 and TMA contain abundant rigid benzene groups, which could limit their application in bridge deck pavement. Thus, exploring a flexible epoxy curing agent is the key to successful application of E51 and TMA in bridge deck pavement. In this study, the main objective of this work is to prepare a flexible polymerized fatty acids (PFA) epoxy curing agent

which can be used in epoxy asphalt fields using EFAME as raw materials. To our knowledge, this is the first report to utilize EFAME as main feedstock to prepare epoxy asphalt. The prepared PFA has many weak-polar aliphatic chain structures, which bestow epoxy asphalt with excellent miscibility. Herein, we emphatically report an ‘epoxy ring opening polymerization and hydrolysis’ strategy to prepare PFA. In the MTA and PFA mixed curing system, however, the cured epoxy matrix system tends to separate from each other because of their different curing speeds. Thus, tong oil maleic tribasic acid (TMTA), another vegetable oil-based curing agent, was also added into the curing system to adjust their curing speeds. Then a series of epoxy asphalt materials were prepared using TMA, PFA, TMTA, E51 and 70# asphalt as raw materials. The compatibility and properties of the prepared epoxy asphalt materials were also investigated. EFAME is eco-friendly chemical feedstock. The utilization of oil resources for preparing epoxy asphalt materials is considered as an alternative way to weaken environmental pollution as well as the dependence on fossil energy.

## **2. Experimental**

### **2.1 Materials**

Epoxy fatty acid methyl ester (EFAME) (epoxy value, 0.34, derived from genetically modified soybean oil) was purchased from Taixing Yuanda Chemical Industry Co., Ltd., China and used as received. Tong oil maleic tribasic acid (TMTA) (acid value, 370) was prepared in our laboratory. E51 epoxy resin, methyl tetrahydrophthalic anhydride (MTA) and DMP-30 accelerant were purchased from Wuxi resins Co., Ltd., China and used as received. NaOH (stabilized, 98%), ethanol

(stabilized, 99%),  $\text{BF}_3 \cdot \text{OEt}_2$  (stabilized, 98%) and  $\text{HCl}$  (stabilized, 98.5%) were purchased from Nanjing Chemical Reagent Co., Ltd., China and used as received. 70# industrial asphalt (softening point, 51.6; ductility, 129.6 cm, 15 °C; needle penetration, 71.4, 25 °C/0.1 mm; SARAs fractions: 10.04 wt% of saturates, 55.91 wt% of aromatics, 26.74 wt% of resins, 7.31 wt% of asphaltenes) was obtained from Ningbo Ruixin polymers Co., Ltd., China and used as received.

## **2.2 Preparation of epoxy asphalt materials**

### **2.2.1 Preparation of polymerized fatty acid methyl ester (PFAME)**

Ring-opening polymerization of EFAME proceeded in a 1-L four-necked round-bottom flask equipped with a mechanical stirrer, a condenser and a thermometer. First, 300.0 g of EFAME and 200.0 g of dioxane were added to the reactor, and then the mixture was heated to 50 °C with a water bath device. Second, 20.1 g of  $\text{BF}_3 \cdot \text{OEt}_2$  was slowly charged into the reactor using a constant-pressure drop funnel, and then the temperature was controlled at 70-80 °C with the water bath device. After that, the reacting system was adjusted and controlled at 50 °C. After 2 h of reaction, 25 mL of ethanol- $\text{H}_2\text{O}$  (1 : 1) was added to the reactor to deactivate the catalyst. Finally, the solvent dioxane and the residual  $\text{H}_2\text{O}$  were removed by vacuum distillation to obtain a highly viscous liquid of PFAME.

### **2.2.2 Preparation of polymerized fatty acid (PFA)**

PFA was prepared via hydrolyzation using the prepared PFAME as raw material. 21.8 g of  $\text{NaOH}$  was dissolved in 205 mL of ethanol- $\text{H}_2\text{O}$  (1:1, V/V), and then the mixture was introduced into a 1-L four-necked round-bottom flask equipped with a mechanical

stirrer and a thermometer. When the mixture was heated to 70 °C, 162.0 g of PFAME was slowly added to the above reaction system with a dropping funnel over half an hour. Reaction continued at 70 °C for 2.0 h. After that, the reacting system was adjusted to pH 2-3 by slowly adding a certain amount of 5 mol/L HCl, and the reaction continued at 70 °C for 1.0 h. After standing for 30 min, the supernatant PFA was taken out. The final product was washed with H<sub>2</sub>O. Finally, the residual H<sub>2</sub>O was removed by vacuum distillation. Then a highly viscous liquid of pure PFA was obtained. Figure 1 shows the typical route of PFA synthesis. The prepared PFA has a viscosity of 5540 mPa·s(NDJ-1 viscosimeter, 25 °C), an acid value of 189(Theoretical values, 192-196), a coloration of 14(Fe-Co colorimeters) and a weight-average molecular weight of 2042(GPC analysis results, M<sub>w</sub>).

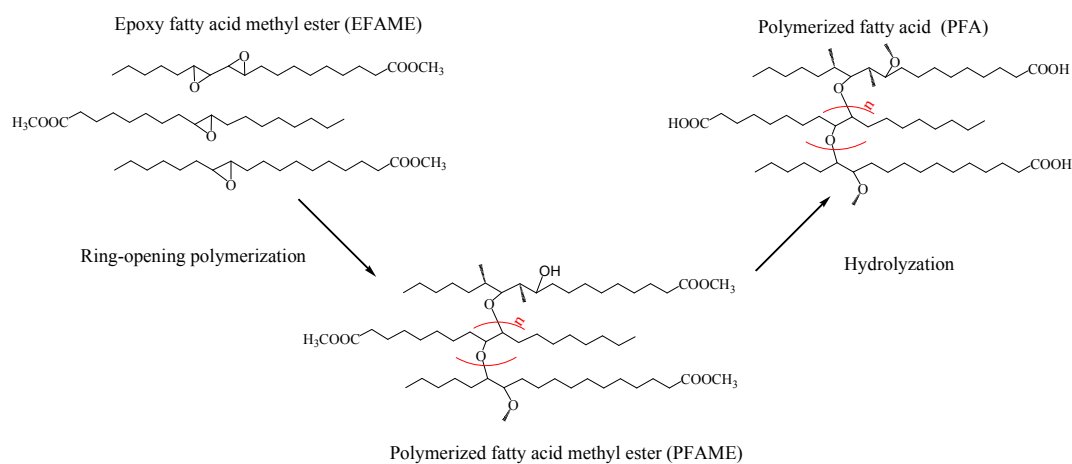


Figure 1 The typical route of PFA synthesis

### 2.2.3 Preparation of epoxy asphalt materials

Table 1 Mixed proportion of different components in epoxy asphalt materials

Formula for mixed curing system	E51 /g	TMTA /g	PFA /g	MTA /g	DMP-30 /g	Total cured system/g (60%)	70# asphalt /g (40%)



MTA70/PFA00/TMTA30	15.00	10.00 <sub>(30%)</sub>	0.00 <sub>(0%)</sub>	8.89 <sub>(70%)</sub>	0.68	34.57	23.05
MTA60/PFA10/TMTA30	15.00	10.00 <sub>(30%)</sub>	3.00 <sub>(10%)</sub>	7.62 <sub>(60%)</sub>	0.71	36.33	24.22
MTA50/PFA20/TMTA30	15.00	10.00 <sub>(30%)</sub>	6.00 <sub>(20%)</sub>	6.35 <sub>(50%)</sub>	0.75	38.10	25.40
MTA40/PFA30/TMTA30	15.00	10.00 <sub>(30%)</sub>	9.00 <sub>(30%)</sub>	5.08 <sub>(40%)</sub>	0.78	39.86	26.57
MTA30/PFA40/TMTA30	15.00	10.00 <sub>(30%)</sub>	12.00 <sub>(40%)</sub>	3.81 <sub>(30%)</sub>	0.82	41.63	27.75

A series of epoxy asphalt materials were prepared by changing the weight ratio of methyl tetrahydrophthalic anhydride (MTA) to PFA. First, a predetermined amount of tong oil maleic tribasic acid (TMTA) and E51 epoxy resin were mixed, and then added with certain amounts of MTA and PFA, and a DMP-30 accelerant (0.2 wt% of the total mixed resin weight). Next, a predetermined amount of 70# asphalt was added. Finally, the obtained mixtures were blended well at 120 °C with a mechanical stirrer until a visually uniform mixture was obtained. The detailed data of the mixed system are listed in Table 1. Cured epoxy asphalt products were prepared by casting the above mixture into a special mould, followed by curing at 120 °C for 3 h. In view of comprehensive performance and cost, all prepared epoxy asphalt materials contained 40 wt% of 70# asphalt and 60 wt% of total weight of E51 epoxy resin and mixed curing agents.

The prepared epoxy asphalt materials were denoted as follows: the mixed curing system MTA60/PFA10/TMTA30 means that 60 wt% of E51 epoxy was cured with MTA, 10 wt% with PFA, and 30 wt% with TMTA.

## 2.3 Characterizations

### 2.3.1 Tensile properties Tests

The liquid mixtures of E51 epoxy resin, mixed curing agents, accelerant and mixed asphalt were transformed into desired solid forms for testing in special moulds

according to the method mentioned above. Tensile properties were measured in accordance with GB/T 25678-2008. The tensile samples were tested by a CMT4303 universal test machine (SANS, China). Tensile test speed was 10mm/min, and test region of the samples was  $4.00\pm 0.10$  mm thick,  $10\pm 0.10$  mm wide, and  $50\pm 0.50$  mm long. Tensile strength and breaking elongation were all measured. Five sample pieces were prepared for each group, and tested at 25 °C.

### **2.3.2 Fourier transform infrared (FTIR) analysis**

Fourier transform infrared (FTIR) analysis was performed using an IS10 spectrometer (Nicolet, USA) by an attenuated total reflectance method. Samples were analyzed as powder or films on a diamond window. Each sample was scanned from 4000 to 400  $\text{cm}^{-1}$ .

### **2.3.3 $^1\text{H-NMR}$ analysis**

$^1\text{H-NMR}$ (300 MHz) spectra were recorded on a Bruker ARX300 spectrometer. The chemical shifts were recorded in ppm (d) relative to tetramethylsilane.

### **2.3.4 Scanning electron microscopy (SEM) analysis**

The samples were fractured after freezing in liquid nitrogen, and then the exposed broken surface was coated with a thin gold layer by using a high vacuum gold sputter at low voltage, after that, the micrographs were observed by magnifying 1,000 or 2,000 times with an S-3400N scanning electron microscopy (Hitachi, Japan) under conventional secondary electron imaging conditions at an accelerating voltage of 20 kV.

### **2.3.5 Dynamic mechanical thermal analysis (DMA)**

The storage modulus( $E'$ ), and loss factor( $\tan\delta$ ) were measured by a Q800 dynamic

mechanical thermal analyzer (TA, USA) in flexural test mode. All samples had a dimension of 60 mm × 10 mm × 4 mm, and were tested from -70 to 80 °C at a heating rate of 3 °C/min and a frequency of 1 Hz.

### 2.3.6 Cure behavior analysis

The cure behavior was studied by non-isothermal DSC analysis methods. Epoxy curing system were measured with a PerkinElmer (USA) Diamond differential scanning calorimeter. All sample were tested from 30 to 260 °C. The heating scanning rate was 10, 20, 30, 40 K/min, respectively.

## 3 Results and discussion

### 3.1 Fourier transform infrared spectroscopy (FTIR) Analysis

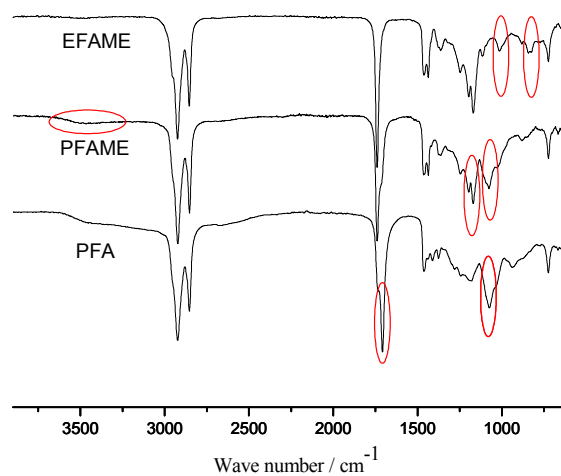


Figure 2 FTIR analysis of EFAME, PFAME and PFA

Figure 2 depicts the FTIR spectra of EFAME, PFAME and PFA. On the spectrum of EFAME, the most specialized characteristic peaks at 1017.8 and 844.9  $\text{cm}^{-1}$  are attributed to the antisymmetric stretching vibration of epoxy group. The sharp and strong peaks at 1194.3 and 1168.5  $\text{cm}^{-1}$  correspond to the overlapped stretching

vibrations of C—O of ester and epoxy groups. The spectrum of PFAME clearly shows the emergence of two absorption peaks at 3501.5 and 1080.3  $\text{cm}^{-1}$ , corresponding to the stretching vibration of hydroxyl and aliphatic ethers, respectively, which indicate the occurrence of ring-opening and polymerization. The overlapped strong peaks at 1194.3 and 1168.5  $\text{cm}^{-1}$  also indicate the occurrence of polymerization. Such weak peak at 3501.5  $\text{cm}^{-1}$  indicates that the prepared PFAME has a high degree of polymerization.

On the spectrum of PFA, the peak at 1712.8  $\text{cm}^{-1}$  is assigned to C=O of carboxyl groups in association state, and the absorption peak at 1736.5  $\text{cm}^{-1}$  corresponds to C=O of ester group which ever exists on the FTIR spectrum of PFAME almost disappear. The peak at 1076.6  $\text{cm}^{-1}$  is assigned to the overlapped stretching vibration absorptions of C—O of carboxyl and epoxy groups, and the peak at 1179.6  $\text{cm}^{-1}$  corresponding to C—O of ester group is greatly weakened. All these changes indicate the occurrence of hydrolyzation of PFAME. Additionally, the appearance of overlapped wide absorption peak at 3500-2500  $\text{cm}^{-1}$  corresponding to O—H of carboxyl groups in association state further confirms the occurrence of hydrolyzation. All these evidence demonstrates the target product PFA has been successfully synthesized.

### 3.2 $^1\text{H-NMR}$ analysis

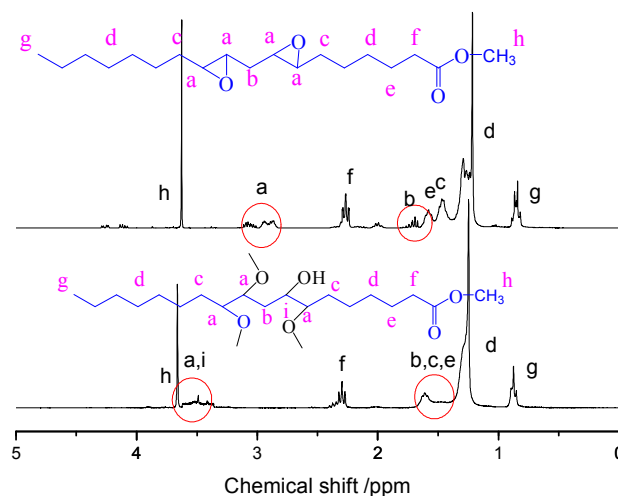


Figure 3  $^1\text{H-NMR}$  spectrum of EFAME and PFAME

In view of the importance of catalytic ring-opening polymerization for preparing PFA, the molecular structures of EFAME and PFAME were further analyzed by using  $^1\text{H-NMR}$ . Figure 5 displays the  $^1\text{H-NMR}$  spectra of EFAME and PFAME. Due to the complexity of the raw material and prepared product, a lot of overlapped peaks were found on the  $^1\text{H-NMR}$  spectra of EFAME and PFAME. For the  $^1\text{H-NMR}$  spectrum of EFAME, the overlapped peaks at 3.10 and 2.90 ppm are assigned to the methine protons on epoxy groups. The main characteristic peaks at about 1.56 ppm are related to the methylene protons next to two epoxy groups, while the characteristic peaks at about 1.56 ppm correspond to the methylene protons next to one epoxy group. The curve of PFAME displays the characteristic peaks at 3.38-3.62 ppm corresponding to the methine protons on the generated ether linkage of  $-\text{CH}-\text{O}-\text{CH}-$ group, and the complexity of this peak indicated the existence of the protons on hydroxyl, which is in accordance with FTIR analysis results. The overlapped characteristic peaks at about 1.61 ppm are assigned to the methylene protons next to ether linkage newly formed and the

methylene protons adjacent to carbonyl groups in meso-position. All characteristic peaks of methylene and methine protons are related to epoxy groups have disappeared, which further confirmed the ring-opening polymerization of epoxy groups under lewis acid condition.  $^1\text{H-NMR}$  analysis results demonstrate that PFAME was successfully synthesized.

### 3.3 Tensile properties

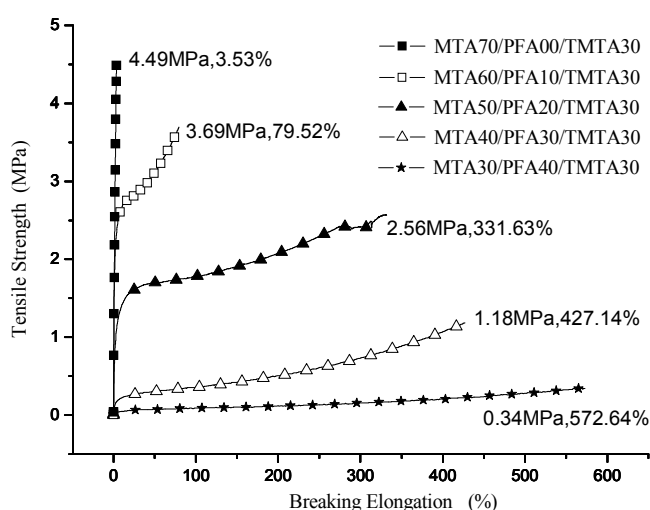


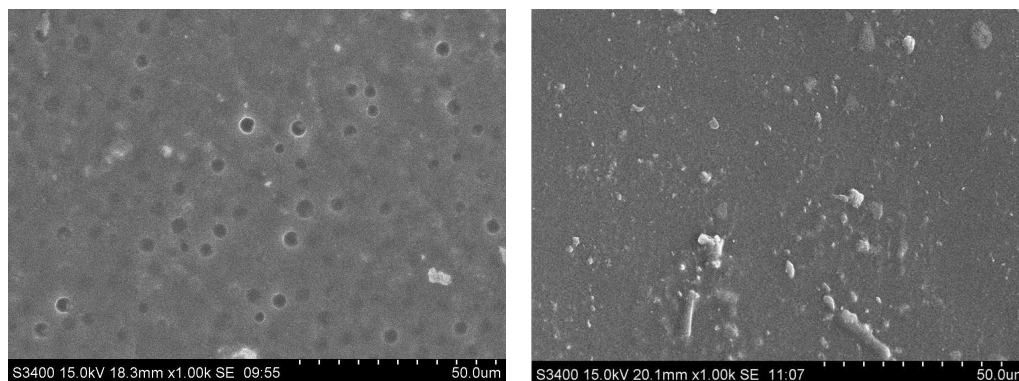
Figure 4 Tensile stress-strain curves of epoxy asphalt composites with different curing systems

Figure 4 shows the typical tensile stress-strain curves of the epoxy asphalt composites obtained from tensile measurements. All stress-strain curves show flexible tensile behavior with no yield stress point but MTA70/PFA0/TMTA30 curing system, indicating those composites containing PFA have the characteristics of flexible materials. The tensile strength of the epoxy asphalt composites generally decreases with the increasing content of PFA, but their breaking elongation changes oppositely, indicating the copolymers' rigidity decreases with the increased PFA content. The tensile strength and breaking elongation of epoxy asphalt composites are decided by the

epoxy-cured systems' cross-linked states and chemical structures, which also change with the variation of mixed proportion of curing agents.<sup>31</sup> For PFA curing agent, its molecule contains multiple carboxyl group and flexible alkyl chain group, which bestow the mixed curing agents with excellent curable activity as well as improve the flexibility of cured system.

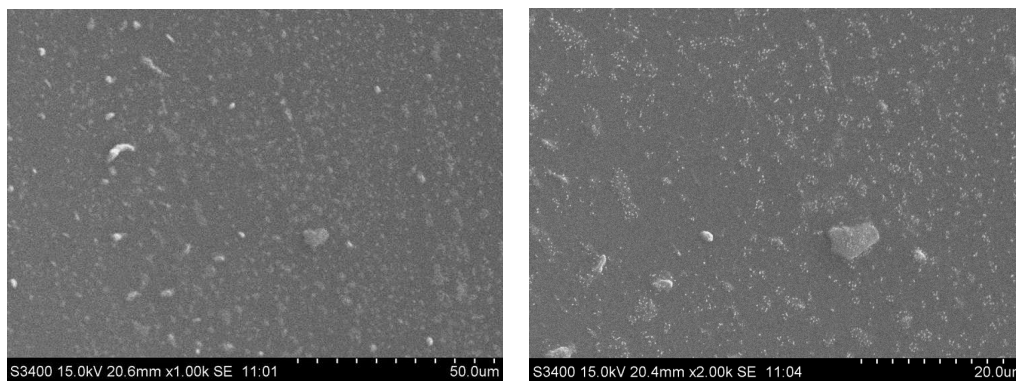
The tensile testing results indicate that its overall mechanical properties are dominated by those branched fatty acids from PFA. More PFA in the compositing system means the materials have higher flexibility. When the PFA curing ability is above 10%, chemical structure is the main factor influencing the composite' tensile strength and breaking elongation, and thus the MTA60/PFA10/TMTA30 cured system shows the high tensile strength of 3.69 MPa, and its breaking elongation at a low level remains 79.52%. With 40% of PFA, the breaking elongation reaches 572.64%, while the tensile strength is only 0.34 MPa, probably because the curing and compositing system contain many branched fatty acids groups, which endow the composites with very high flexibility.

### 3.4 Morphologic Properties



(a) MTA70/PFA00/TMT30×1,000SE

(b) MTA50/PFA20/TMT30×1,000 SE



(c) MTA30/PFA40/TMT30×1,000 SE

(d) MTA30/PFA40/TMT30×2,000 SE

Figure 5 SEM images of liquid-nitrogen brittle fracture surface of epoxy asphalt composites

Figure 5 depicts the scanning electron microscope (SEM) images of liquid-nitrogen brittle fracture surface of epoxy asphalt composites in different curing systems. The relatively smooth fracture indicates that all the curing agents had formed a perfect cross-linked structure system with E51 epoxy resin after cross-linking polymerization, and formed the continuous phase of composites. The fracture surface of the MTA and TMT cured system showed a clear phase-separation structure, and abundant globular cavities were dispersed in the continuous phase (Fig. 5a). These cavities are less than 5  $\mu\text{m}$  and distributed uniformly in nature. Their formation might be attributed to the decomposition and evaporation of MTA components during the curing process, as well as the incompatibility between some components of asphalt and the cured epoxies using MTA, and figures 5 b, c, also show little interphase separation. Cured E51 epoxies formed a composite matrix whereas asphalt formed a dispersed phase. With the increased PFA content, the dispersion of asphalt becomes more even, indicating the excellent compatibility between the PFA curing system and asphalt. In the MTA30/PFA40/TMT30 curing system, no obvious globular cavities were seen on the



fracture surface. In the copolymerized system, under certain temperature and with the addition of the accelerant, the molecular chains of MTA, PFA, and TMT could covalently link with E51 epoxy resin on the cross-linking point and join all molecular chains together.

### 3.5 Dynamic mechanical analysis (DMA)

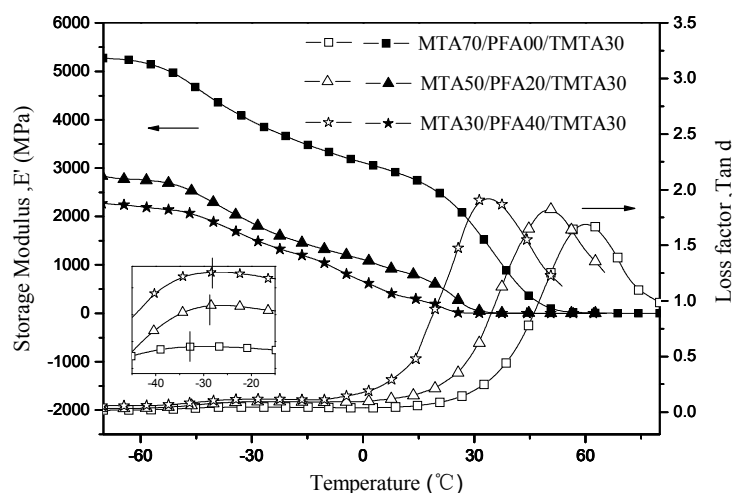


Figure 6 DMA traces of epoxy asphalt composites with different curing systems

The dynamic mechanical behaviors of the samples were studied. The DMA curves including storage modulus ( $E'$ ) and loss factors ( $\tan\delta$ ) are summarized in Figure 6. All  $E'$  curves display a similar trend:  $E'$  decreases sharply at two stages from -45 to -15 °C and from -15 to 50 °C. Below 15 °C, all composites exhibit the properties of a glassy state, in this case all the molecular segmental motions are frozen, and thus  $E'$  remained at a high level from 500 to 5500 MPa. With increasing temperature, the frozen segmental structure begins to relax gradually, and above 60 °C, all the  $E'$  values are all close to a constant below 5 MPa, indicating higher molecular chain motions in the

copolymerized system. In addition,  $E'$  decreases with the increased PFA content. It is well known that the mechanical and thermal properties of cured thermosets are very sensitive to the chemical structure nature of each component in the copolymerized system.<sup>32</sup> The proportion of flexible long-chain structure in the copolymerized system increases with the increased PFA content, while the proportion of rigid benzene ring structure existing in MTA decreases. High content of flexible long-chain structure can bestow materials with low rigidity, and thus the composites have low  $E'$ , which is similar to the composites' mechanical properties.

All  $\tan\delta$  curves in Figure 6 display two peaks at  $-35 \sim -25$  and  $30 \sim 60$  °C, respectively, which indicate two different phases. It is known that glass transition temperature ( $T_g$ ) depends on several factors such as chemical structure, components, and cross-linked state for thermosetting composites.<sup>33</sup> The weak peak at low temperature might be assigned to the asphalt phase in the composites, and the peak at high temperature probably corresponds to the molecular structure relaxation of the continuous phase of cured epoxies. At low temperature, with the increased PFA content, the glass  $T_g$  corresponding to  $\tan\delta$  peak increased. However, the main  $\tan\delta$  peak at high temperature changed oppositely, and the corresponding  $T_g$  shifted greatly to low temperature. These changing trends of  $T_g$  indicate the excellent compatibility between the PFA cured system and asphalt. The intensity of all  $\tan\delta$  peaks increases with the increased PFA content, indicating that a higher content of flexible long-chain structure could more effectively improve the chain mobility of the cured system, thus the  $\tan\delta$  curves show wider and lower peak. Less and less energy was needed to relax the molecular

chains of each cured component with the increased PFA content, resulting in temperature decline corresponding to the  $\tan\delta$  peak ( $T_g$ ) at high temperature. Therefore, when the cured system contains the highest content of PFA (40% curing ability), the composite displays the lowest main  $T_g$  of 34.4 °C. The possible molecular interactions diagram between cured matrix and asphalt is shown in Figure 7

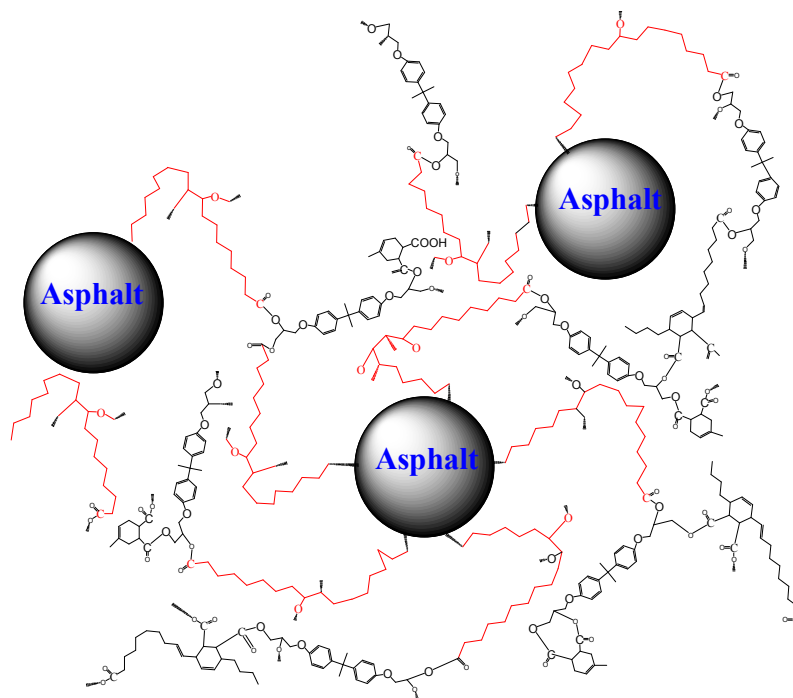


Figure 7 Possible molecular interactions diagram between cured matrix and asphalt

### 3.6 Comprehensive properties comparison

Table 2 Comprehensive properties comparison

Properties	<sup>a</sup> Technical requirements	MTA50/PFA20/TMTA30 curing system (40 wt% of asphalt)	Product from ChemCo Systems Inc. (40 wt% of asphalt)	Test methods
Tensile strength (MPa)	$\geq 1.52$	2.56	2.45	ASTM D638
Breaking elongation(%)	$\geq 190$	331.63	236.01	ASTM D638
Thermosetting character	Unmelted	Unmelted	Unmelted	Place on iron plate at 300°C
Glass-transition	—	48.2	15.20	DMA analysis

temperature  $T_g$  ( $^{\circ}\text{C}$ )

Rate of water absorption (%)	$\leq 0.3$	0.12	0.10	ASTM D4469-11
------------------------------	------------	------	------	---------------

<sup>a</sup> Technical requirements of bridge deck paving for epoxy asphalt. <sup>34</sup>

The properties of the epoxy asphalt materials are listed in Table 2. The comprehensive properties of the product from ChemCo Systems Inc. were also tested for comparison. Clearly, the MTA50/PFA20/TMTA30 curing system shows excellent comprehensive properties (Table 2), since all performance parameters meet the technical requirements for bridge deck paving. This system particularly owns excellent tensile properties for bridge deck paving. Our newly-prepared product has higher tensile strength and breaking elongation compared with the ChemCo product. The new curing system also possesses a higher  $T_g$ , which allows it to be used safely in hot summer. The MTA50/PFA20/TMTA30 curing system has a low water absorption rate of 0.12%. In this system, lots of hydrophobic groups from vegetable oil were added into the cross-linking structure, which bestow them with excellent hydrophobic property.

### 3.7 Cure behavior analysis of the optimal curing system for bridge paving

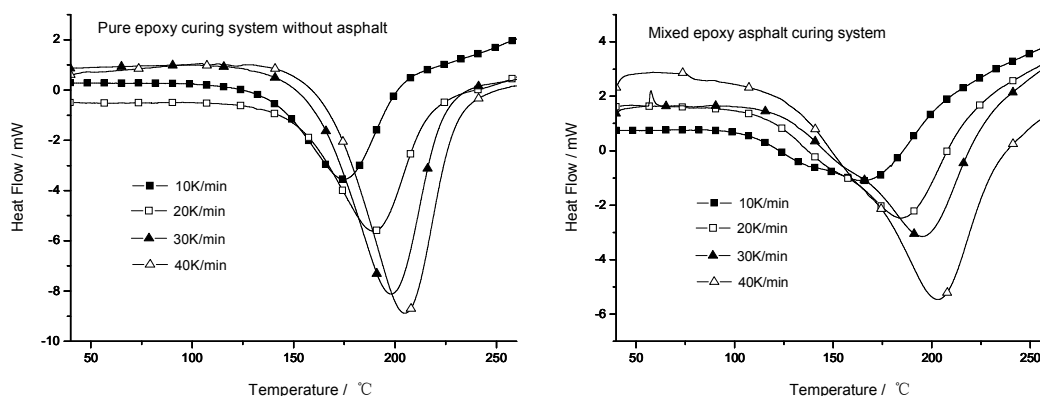


Figure 8 DSC analysis curves of pure epoxy without asphalt and mixed epoxy asphalt curing system

The MTA50/PFA20/TMTA30 curing system shows excellent comprehensive properties,

which can meet the technical requirements for bridge deck paving. Thus, we further investigated the curing behavior of this curing system by DSC non-isothermal curing kinetic methods, including pure epoxy without asphalt and the mixed epoxy asphalt curing system. All DSC analysis curves are shown in Figure 8, and the temperatures at which thermal cure takes place in the different curing systems' thermal events are shown in Table 3. All DSC heating flow curves show a single exothermic peak. Along with the increasing heating rate, the initial( $T_i$ ), peak( $T_p$ ) and end( $T_e$ ) curing reaction temperatures increase and the exothermic peaks become sharper, indicating a much more focused exothermic process and a quicker curing reaction. As the heating rate was raised,  $dH/dt$  increased. That is to say, with the increase of heating effects in unit time, its thermal inertia and the temperature difference both increased, and thus, the exothermic peak of the curing reaction shifted to high temperature. The curve of pure epoxy curing system shows a larger curing exothermic peak corresponding to higher  $\Delta H(60\%)$  in Table 3 compared with the mixed epoxy asphalt curing system at the same heating flow rate. Asphalt almost did not participate in the curing reaction, but reduced the contact between curing agents and epoxy resin, and then inhibited their curing reaction, thus the mixed epoxy asphalt curing system released less heat and showed a flat exothermic peak on DSC curve.

Table 3 Detailed DSC analysis data of different curing systems

Curing systems	$\beta$ (k/min)	$T_i$ (°C)	$T_p$ (°C)	$T_e$ (°C)	$\Delta H$ / (J/g)
Pure epoxy curing	10	140.33	175.13	200.83	-121.90/-73.14 <sub>(60%)</sub>
system without	20	153.59	189.52	215.63	-112.48/-67.49 <sub>(60%)</sub>
asphalt	30	158.73	197.30	223.22	-105.80/-63.48 <sub>(60%)</sub>

	40	166.31	204.18	229.68	-88.88/-53.33 <sub>(60%)</sub>
Mixed epoxy asphalt curing system	10	112.18	168.43	190.06	-69.03
	20	123.19	184.98	217.69	-63.76
	30	148.23	195.03	225.24	-53.04
	40	156.16	201.98	232.21	-50.49

The key kinetic parameters of the curing reaction, with special reference to activation energy ( $E_a$ ), can be calculated using various computational methods. In our study,  $E_a$  was determined by non-isothermal DSC analysis with Kissinger equation (Equation 1) as follows.

Kissinger equation:<sup>35</sup>

$$\ln\left(\frac{\beta}{T_p^2}\right) = \ln\left(\frac{AR}{E_a}\right) - \left(\frac{E_a}{RT_p}\right) \quad \text{Equation 1}$$

where:  $\beta$  is heating scanning rate (K/min),  $T_p$  is peak temperatures on DSC curve (K),  $A$  is pre-exponential factor ( $s^{-1}$ ),  $R$  is ideal gas constant (8.314 J/mol·K) and  $E_a$  is curing reaction activation energy (kJ/mol).

The standard linear regression equations between  $-\ln(\beta/T_p^2)$  and  $1/T_p$  were obtained with linear regression method. Based on these equations, we computed the curing  $E_a$  in different curing systems. The equations, lines and  $E_a$  are shown in Figure 8. The linear equation correlation coefficients of pure epoxy and mixed epoxy asphalt curing systems are 0.9987 and 0.9996, respectively, which reach extremely high measuring levels. The results show that standard linear curves are of very good linear correlation which can accurately measure curing  $E_a$  of different curing systems. The pure epoxy curing system without asphalt had a higher  $E_a$  than the mixed epoxy asphalt curing system (77.8801 vs. 64.2233 kJ/mol), indicating that the curing reaction is more easily to occur in the mixed

epoxy asphalt system. Although the mixed epoxy asphalt curing system contained 40 wt% of asphalt, its  $E_a$  was higher than the theoretical value by comparing with the pure epoxy curing system without asphalt. The addition of asphalt reduced the molecular contacting opportunity between epoxy resin and curing agents, and thus more energy was needed, corresponding to a higher  $E_a$  than the theoretical value. In addition, some curing reactions could occur between reactive groups of asphalt and epoxy resin. These two factors might jointly influence the  $E_a$  of curing system, and thus  $E_a$  is higher in the mixed epoxy asphalt curing system.

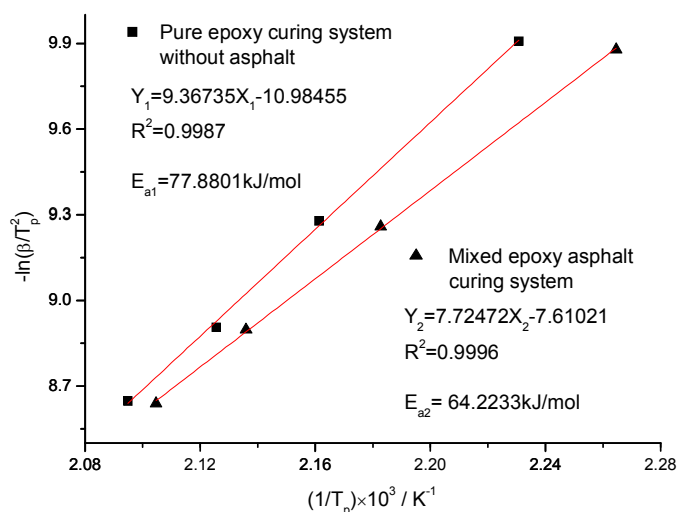


Figure 9 Standard linear regression equations of different curing systems

#### 4. Conclusions

FTIR analysis demonstrated that a novel PFA epoxy curing agent has been successfully synthesized. The even dispersion of asphalt on liquid-nitrogen brittle fracture surface indicated excellent compatibility between the PFA cured system and asphalt. The weight ratios of PFA in the curing system significantly affected the mechanical

properties of the prepared epoxy asphalt. DMA revealed the same result as micro-morphologic investigation, and the changing trend of  $T_g$  indicates the excellent compatibility between the PFA cured system and asphalt. Prepared toughened curing system can meet technical requirements for bridge deck paving due to its excellent comprehensive properties. The  $E_a$  of the optimal toughened mixed epoxy asphalt curing system was higher and close to the value of pure epoxy curing system without asphalt. This study presents a perfect application of the flexible aliphatic chain structure in epoxy asphalt field for paving bridges.

### Acknowledgements

This research project was supported by international cooperation and exchanges project(grant number: 2011DFA32440).

### Reference:

- [1] A. García and M.N. Partl, *Appl. Energ.*, 2014,**119**, 431-437.
- [2] A. Modarres and H. Hamed, *Mater. Design.*, 2014, **61**, 8-15
- [3] X. Yu, M. Zaumanis, S. Santos and L. D. Poulikakos, *Fuel*, 2014, **135**, 162-171.
- [4] S. Cui, B. R. K. Blackman, A. J. Kinloch and A. C. Taylor, *Int. J. Adhes. Adhes.*, 2014, **54**, 100-111.
- [5] H. C. Dan, L. H. He, J. F. Zou, L. H. Zhao and S. Y. Bai, *Cold. Regi. Sci. Technol.*, 2014, **104-105**, 7-13.
- [6] B. Gómez-Meijide and I. Pérez, *Mater. Design*, 2014, **57**, 520-527.
- [7] W. Kongkitkul, N. Musika, C. Tongnuapad, P. Jongpradist and S. Youwai, *Soils Found.*, 2014, **54**, 94-108.



- [8] A. M. M. Abd El Rahman, M. EL-Shafie and S. A. El Kholly, *Egypt. J. Petrol.*, 2012, **21**, 139-147.
- [9] H. Abd El-Wahab, A. M. M. Saleh, M. A. Wassel, G. Elkady, N. S. Khalaf and S. Ahmed, 2013. *Prog. Org. Coat.*, 2013, **76**, 1363-1368.
- [10] J. F. Su, E. Schlangen and J. Qiu, *Powder Technol.*, 2013, **235**, 563-571.
- [11] T. W. Kim, J. Baek, H. J. Lee and J. Y. Choi, *Constr. Build. Mater.*, 2013, **48**, 908-916.
- [12] F. Zhang and J. Yu, *Constr. Build. Mater.*, 2010, **24**, 410-418.
- [13] M. S. Sureshkumar, S. Filippi, G. Polacco, I. Kazatchkov, J. Stastna and L. Zanzotto, *Eur. Polym. J.*, 2010, **46**, 621-633.
- [14] M. A. Vargas, M. A. Vargas, A. Sánchez-Sólis, and O. Manero, *Constr. Build. Mater.*, 2013, **45**, 243-250.
- [15] Y. Wang, J. Ye, Y. Liu, X. Qiang and L. Feng, *Constr. Build. Mater.*, 2013, **41**, 580-585.
- [16] B. Yao, G. Cheng, X. Wang, C. Cheng and S. Liu, *Constr. Build. Mater.*, 2013, **48**, 540-547.
- [17] Z. Qian, L. Chen, C. Jiang and S. Luo, *Constr. Build. Mater.*, 2011, **25**, 3117-3122.
- [18] Y. Xiao, M. F. C. van de Ven, A. A. A. Molenaar, Z. Su and K. Chang, *Constr. Build. Mater.*, 2013, **41**, 516-525.
- [19] D. Arslan, M. Gürü and M. Kürşat Çubuk, *Cold. Reg. Sci. Technol.* 2013, **85**, 250-255.
- [20] Y. Kang, F. Wang and Z. Chen, *Chem. Eng. J.*, 2010, **164**, 230-237.

- [21] B. Kaur, H.S. Oberoi and B.S. Chadha, *Bioresour. Technol.*, 2014, **156**, 100-107.
- [22] T. Saito, J. H. Perkins, D. C. Jackson, N. E. Trammel, M. A. Hunt and A. K. Naskar, *RSC Adv.*, 2013, **3**, 21832-21840
- [23] T. Witoon, S. Bumrungsalee, P. Vathavanichkul, S. Palitsakun, M. Saisriyoot and K. Faungnawakij, *Bioresour. Technol.*, 2014, **156**, 329-334.
- [24] M. Kashif and S. Ahmad, *RSC Adv.*, 2014, **4**, 20984-20999
- [25] A. S. Aamer, H. Fariha, H. Abdul and A. Safia, *Biotechnol. Adv.*, 2008, **26**, 246-265.
- [26] T. M. Lacerda, A. J. F. Carvalho and A. Gandini, *RSC Adv.*, 2014, **4**, 26829-26837
- [27] C. C. Ting, and C. C. Chen, *Measurement.*, 2011, **44**, 1337-1341.
- [28] A. Adhvaryu and S. Z. Erhan, *Ind. Crops Prod.*, 2002, **15**, 247-254.
- [29] C. Bueno-Ferrer, M. C. Garrigós and A. Jiménez, *Polym. Degrad. Stab.*, 2010, **95**, 2207-2212.
- [30] J. Gilbert, M. J. Shepherd, J. R. Startin and J. Eagles, *Chem. Phys. Lipids.*, 1981, **28**, 61-68.
- [31] T. F. Scott, W. D. Cook and J. S. Forsythe, *Eur. Polym. J.*, 2002, **38**, 705-716.
- [32] S. Li, J. Xia, M. Li and K. Huang, *J. Am. Oil. Chem. Soc.*, 2013, **90**, 695-706.
- [33] S. Wang, J. Wang, Q. Ji, A.R. Shultz, T.C. Ward and J.E. McGrath, *J. Polym. Sci. Pol. Phys.*, 2000, **38**, 2409-2421.
- [34] Z. Qian, C. Chen, C. Jiang and A. F. Smit, *Constr. Build. Mater.*, 2013, **48**, 516-520.
- [35] H. E. Kissinger, *Anal. Chem.*, 1957, **29**, 1702-1706.